2016

The interferon-stimulated gene IFITM3 restricts West Nile virus infection and pathogenesis

Matthew J. Gorman
Washington University School of Medicine

Subhajit Poddar
Washington University School of Medicine

Michael Farzan
Washington University School of Medicine

Michael S. Diamond
Washington University School of Medicine

The interferon-stimulated gene IFITM3 restricts West Nile virus infection and pathogenesis

Matthew J. Gorman[1], Subhajit Poddar[1], Michael Farzan[5], and Michael S. Diamond[1,2,3,4,]

Departments of Pathology & Immunology[1], Medicine[2], Molecular Microbiology[3], and the Center for Human Immunology and Immunotherapy Programs[4], Washington University School of Medicine, St Louis, MO 63110 USA. Department of Immunobiology and Microbial Sciences, The Scripps Research Institute[5], Jupiter, Florida 33458.

Corresponding author: Michael S. Diamond, M.D., PhD, Departments of Medicine, Molecular Microbiology and Pathology & Immunology, Washington University School of Medicine, 660 South Euclid Avenue, Box 8051, St Louis. Missouri 63110. Tel: 314-362-2842, Fax: 314-362-9230, Email: diamond@borcim.wustl.edu

Running title: IFITM3 restricts WNV pathogenesis

Figures: 7

ABSTRACT

The interferon induced transmembrane protein (IFITM) family of proteins inhibit infection of several different enveloped viruses in cell culture by virtue of their ability to restrict entry and fusion from late endosomes. As few studies have evaluated the importance of IFITM3 *in vivo* in restricting viral pathogenesis, we investigated its significance as an antiviral gene against West Nile virus (WNV), an encephalitic flavivirus, in cells and mice. *Ifitm3*$^{-/-}$ mice were more vulnerable to lethal WNV infection, and this was associated with greater virus accumulation in peripheral organs and central nervous system tissues. As no difference in viral burden in the brain or spinal cord was observed after direct intracranial inoculation, Ifitm3 likely functions as an antiviral protein in non-neuronal cells. Consistent with this, *Ifitm3*$^{-/-}$ fibroblasts but not dendritic cells resulted in higher yields of WNV in multi-step growth analyses. Moreover, trans-complementation experiments showed that Ifitm3 inhibited WNV infection independently of Ifitm1, Ifitm2, Ifitm5, and Ifitm6. Beyond a direct effect on viral infection in cells, analysis of the immune response in WNV-infected *Ifitm3*$^{-/-}$ mice showed decreases in the total number of B cells, CD4^{+} T cells, and antigen-specific CD8^{+} T cells. Finally, bone marrow chimera experiments demonstrated that Ifitm3 functioned in both radioresistant and radiosensitive cells, as higher levels of WNV were observed in the brain only when Ifitm3 was absent from both compartments. Our analyses suggest that Ifitm3 restricts WNV pathogenesis likely through multiple mechanisms including the direct control of infection in subsets of cells.

41 **IMPORTANCE**

42 As part of the mammalian host response to viral infections, hundreds of interferon-
43 stimulated genes (ISGs) are induced. The inhibitory activity of individual ISGs varies depending
44 on the specific cell type and viral pathogen. Among ISGs, the interferon-induced
45 transmembrane proteins (*IFITM*) genes have been reported to inhibit multiple families of viruses
46 in cell culture. However, few reports have evaluated the impact of IFITM genes on viral
47 pathogenesis *in vivo*. In this study, we characterized the antiviral activity of Ifitm3 against West
48 Nile virus (WNV), an encephalitic flavivirus, using mice with a targeted gene deletion of *Ifitm3*.
49 Based on extensive virological and immunological analyses, we determined that Ifitm3 protects
50 mice from WNV-induced mortality by restricting virus accumulation in peripheral organs and
51 subsequently, in central nervous system tissues. Our data suggest that Ifitm3 restricts WNV
52 pathogenesis by multiple mechanisms and functions in part, by controlling infection in different
53 cell types.

54

INTRODUCTION

The interferon (IFN) induced transmembrane protein (IFITM) genes consist of a family of related proteins; *Ifitm1, 2, 3, 5, 6, 7,* and *10* in mice and *IFITM1, 2, 3, 5,* and 10 in humans (1, 2). The expression of several IFITM genes, (e.g., IFITM1, 2, and 3) can be induced by type I, II, or III IFNs (3, 4). Although initial studies described possible roles of IFITM1, IFITM2, and IFITM3 in development, apoptosis, cell proliferation, and cell signaling (5–13), a subsequent report suggested that ectopic expression of IFITM1 in mouse L cells could restrict infection of vesicular stomatitis virus (VSV) (14). A decade later, gene silencing and ectopic expression studies established that IFITM proteins have antiviral activity in cell culture against members of the *Flaviviridae*, *Orthomyxoviridae*, *Filoviridae*, *Rhabdoviridae*, *Retroviridae*, *Bunyaviridae*, *Reoviridae*, *Togaviridae,* and *Paramyxoviridae* families (15–28). Nonetheless, some enveloped and non-enveloped viruses appear resistant to the actions of IFITM proteins including arenaviruses, papillomaviruses, cytomegaloviruses, and adenoviruses (16, 17, 29).

IFITM proteins are transmembrane proteins. Although their precise membrane topology remains uncertain (5, 6, 15, 30–36), recent studies suggest that they are type II membrane proteins (35–37). Moreover, the cellular sublocalization of the IFITM proteins varies among family members, with IFITM1 expressed primarily at the plasma membrane, and IFITM2 and IFITM3 colocalizing predominantly with late endosomes (20, 32). Based on the cellular localization and effects on specific steps in viral lifecycles, IFITM1, IFITM2, and IFITM3 appear to restrict fusion and uncoating of viruses into the cytoplasm (33, 38, 39), with different IFITM proteins inhibiting specific viruses in distinct membrane compartments. Despite the intensive study of the IFITM proteins in cell culture, the precise mechanism of restriction of viral fusion has remained elusive. It has been suggested that IFITM proteins can increase cholesterol accumulation in endosomes, alter membrane fluidity, or make fusion events energetically unfavorable (17, 33, 38, 40). IFITM1, IFITM2, and IFITM3 also can become incorporated into virions and restrict viral infection, as has been demonstrated with HIV (41, 42).

Although IFITM proteins can restrict infection of many viruses in cell culture, their importance *in vivo* in the context of a complex IFN response with hundreds of other interferon-stimulated genes (ISGs) remains less well characterized. Two publications have reported that *Ifitm3*$^{-/-}$ mice are more susceptible to influenza A virus (IAV) infection (3, 43). These studies described increased IAV titers in the lung, increased pathology, and decreased CD4^{+} T cells, CD8^{+} T cells, and NK cells in *Ifitm3*$^{-/-}$ compared to WT mice. One of these studies described a human polymorphism in *IFITM3*, (SNP-rs12252-C) that results in an altered splice acceptor site, which truncates the N-terminal 21 amino acids of IFITM3. This truncated IFITM3 protein showed altered cellular localization and reduced antiviral activity against IAV (32, 43, 44). A second study demonstrated that CD8^{+} resident memory T cells expressed high levels of *Ifitm3* in the lung following IAV infection, and that *Ifitm3* expression was important for memory T cell survival against virus rechallenge (45). Ifitm3 also reportedly has an antiviral role against respiratory syncytial virus *in vivo*, as *Ifitm3*$^{-/-}$ mice sustained higher viral burden in the lungs (46). To date, no studies have described an antiviral role of Ifitm3 *in vivo* apart from viruses that preferentially infect the lung.

West Nile virus (WNV) is a neurotropic, mosquito-transmitted, positive-stranded, enveloped RNA virus in the *Flaviviridae* family, which includes several viruses of global concern such as Dengue (DENV), Zika (ZIKV), yellow fever (YFV), and Japanese encephalitis (JEV) viruses. Whereas most infections with WNV in humans are asymptomatic, ~30% develop a febrile illness, which can progress to severe neurological disease including meningitis, flaccid paralysis, encephalitis, and death (47, 48). Several studies have established that IFN signaling and induction of downstream antiviral effector proteins (e.g., IFIT2, viperin, PKR, RNAse L, and Ifi27l2a) restrict the tropism and dissemination of WNV (49–52). Here, we examined the role of Ifitm3 *in vivo* in restricting infection of WNV using *Ifitm3*$^{-/-}$ mice. Extensive virological and immunological analysis revealed that *Ifitm3*$^{-/-}$ mice were more vulnerable to WNV infection with greater lethality, higher viral burden, and altered immune induction. Our study demonstrates a

contribution of Ifitm3 to controlling WNV in peripheral organs prior to dissemination to the brain and infection and injury of target neuron populations.

MATERIALS AND METHODS

Ethics statement. This study was carried out in strict accordance with the recommendations in the Guide for the Care and Use of Laboratory Animals of the National Institutes of Health. The protocols were approved by the Institutional Animal Care and Use Committee at the Washington University School of Medicine (Assurance Number: A3381-01). Dissections and footpad injections were performed under anesthesia that was induced and maintained with ketamine hydrochloride and xylazine, and all efforts were made to minimize suffering.

Virus propagation. The WNV strain New York 1999 (53, 54) was passaged in Vero cells to generate a mammalian cell derived stock. The WNV strain from Madagascar (DakAnMg 798, WNV-MAD) was isolated in 1978 and also passaged in Vero cells (55). Titration of viral stocks was performed using a focus-forming assay as described previously (56).

Mouse experiments and tissue preparation Wild-type (WT) C57BL/6 (000664) or B6.SJL (002014) mice were purchased from Jackson Laboratory. *Ifitm3*$^{-/-}$ mice were generated previously (57), backcrossed using speed congenics onto a C57BL/6J background, and bred in a pathogen free animal facility at the Washington University School of Medicine. Eight to ten week-old age and sex-matched mice were used. Mice were infected via a subcutaneous (10^2 FFU in 50 µl) or intracranial (10^1 FFU in 10 µl) route with virus diluted in PBS. For survival studies, infected mice were monitored for 21 days. For viral burden studies, at specified time points after infection, serum was collected and animals were perfused with 20 ml of PBS. Subsequently, the spleen, kidney, draining lymph node, brain, and spinal cord were harvested, weighed, homogenized by bead dissociation using a MagNA Lyzer (Roche). Virus was titered by plaque assay on Vero cells (58, 59) or levels of viral RNA were measured by qRT-PCR as described previously (49, 60).

Measurement of WNV-specific antibodies. WNV-specific IgM and IgG titers were determined by an ELISA using purified WNV E protein as described previously (61). Focus

136 reduction neutralization assay were performed on Vero cells after mixing serial dilutions of
137 serum with a fixed amount (10^2 FFU) of WNV (56).

138 **Analysis of cellular immune responses**. Splenocytes were harvested from WT or
139 *Ifitm3*$^{-/-}$ mice on day 7 or 8 after WNV infection. Lymphocyte populations were stained using
140 anti-CD3-V500 (560711; BD Bioscience), anti-CD8α- or anti- CD8β-Percp Cy5.5 (100734;
141 Biolegend), anti-CD19-AlexaFluor700 (115528; Biolegend), anti-CD4-BV421 (100437;
142 Biolegend), anti-granzyme B (GRB04; Invitrogen), and tetramers specific for a D^b-restricted
143 immunodominant peptide in NS4B (62). Brains were harvested from WT or *Ifitm3*$^{-/-}$ mice on day
144 8 after WNV infection. CNS leukocytes were isolated by Percoll gradient centrifugation as
145 described previously (62, 63) and stained with the antibodies and tetramer described above in
146 addition to anti-CD11b-PE-Cy7 (101216; Biolegend) and anti-CD45-BV605 (103139;
147 Biolegend). Cells were analyzed on a BD LSRII flow cytometer and data were processed using
148 FlowJo software.

149 To examine intracellular cytokine production by $CD4^+$ and $CD8^+$ T cells, anti-CD3 or
150 antigen-specific peptide restimulation was performed (62). In brief, splenocytes were isolated
151 and stimulated with anti-CD3 (100207; Biolegend), the immunodominant NS4B peptide, or no
152 stimulation. Cells were incubated for 6 h at 37°C in the presence of brefeldin A and then fixed
153 and permeablized using the FoxP3/Transcription Factor Staining Buffer set (00-5523-00;
154 eBioscience). Subsequently, cells were stained with anti-CD4-BV421 (100437; Biolegend), anti-
155 CD8β-PerCP-Cy5.5 (126609; Biolegend), anti-CD19-AlexaFluro700 (115528; Biolegend), anti-
156 IFN-γ-APC (51-73-1182; eBioscience), and anti-TNF-α-PE (506306l Biolegend) antibodies and
157 analyzed.

158 **Primary cell isolation and infection**. Primary macrophages (Mϕ), dendritic cells (DCs),
159 and mouse embryonic fibroblasts (MEFs) were generated from WT and *Ifitm3*$^{-/-}$ mice as
160 described (64). For single-step and multi-step growth curves, cells were infected at a multiplicity

of infection (MOI) of 5 and 0.01, respectively. In some experiments, cells were pretreated with IFN-β (12400-1; PBL Assay Science) for 16 h before infection. Viral supernatants were harvested and titered using a focus-forming assay.

Transformation of MEFs. MEFs were transfected with the plasmid SV2, which encodes for the large T antigen of SV40 polyoma virus (65). Cells were passaged ~10 times and used for subsequent experiments.

Trans-complementation of MEFs. ***(a) Production of pFCIV-containing lentivirus.*** 293T cells were seeded at 5 x 10^6 cells per well in a 6 well plate. One day later, cells were transfected with 0.4 µg of pMD.2, 0.8 µg of pSPAX2, and 0.8 µg of pFCIV-c-Myc-Ifitm3 or pFCIV-c-Myc-Firefly luciferase using FuGENE (Roche) according to the manufacturer's instructions (66, 67). Two to three days after transfection, lentivirus was collected from the supernatant of cells, centifruged at 1,000 x g for 10 min at 4°C to remove cellular debris, and then stored at -80°C. ***(b) Generation of MEF transfectants.*** Transformed MEFs were seeded at 0.5 x 10^4 cells per well in a 96 well plate. Six hours after plating, 100 µl of lentivirus + 1 µg polybrene (sc-134220; Santa Cruz Biotech) were added to each well and cells were spinoculated at 1,000 x g, for 30 min at 24°C. Six hours later, lentivirus was removed and replaced with DMEM containing 10% FBS. Cells were passaged and expanded into a T-75 tissue culture flask. Transduced cells were sorted for GFP expression (pFCIV encodes for GFP under a IRES promoter) on a BD FACsAria II flow cytometer. Cells were passaged five times to confirm stable expression by GFP expression and c-Myc tagged protein expression using flow cytometery and then used for subsequent experiments.

Western blotting of Ifitm3 expression. WT or *Ifitm3*$^{-/-}$ MEFs, or *Ifitm3*$^{-/-}$ MEFs trans-complemented with c-Myc-Ifitm3 were seeded at 5 x 10^4 cells per well in a 24 well plate. Cells were stimulated with or without 10 U/mL of IFN-β for 16 h at 37°C. Cells were washed with PBS and then lysed in 200 µL of RIPA buffer with protease inhibitors (Cell Signaling 9806S). Cellular

debris was removed from the sample by centrifugation at 10,000 x g for 10 min at 4°C. The clarified supernatant was resuspended in 4x LDS sample buffer (NuPAGE NP0008), boiled (5 min at 90°C), and then electrophoresed on a 12% Bis-TRIS gel (NuPAGE NP0343BOX) at 200 V for 40 min in MES buffer (NuPAGE NP0002). Protein was transferred to a PVDF membrane (Invitrogen IB24002) using an Iblot2 (Life Technologies IB21001) with a standard 7-minute transfer. A 1:1,000 dilution of mouse anti-β-actin (Protein Tech 11714-1-AP) and rabbit anti-Ifitm3 (Cell Signaling 3700) was prepared in TBS-T + 4% milk and used to stain the membrane overnight at room temperature. Subsequently, after washing, a 1:10,000 dilution of donkey anti-mouse IRDye 800 (LI-COR 925-32212) or anti-rabbit IRdye 680 (LI-COR 926-68073) was prepared in TBS-T + 4% milk and used to stain the membrane for 2 h at room temperature. An Odyssey machine (LI-COR Biosciences) was used to visualize the bands on the membrane.

Infection of MEFs. WT, gene deletion, and trans-complemented MEFs were seeded at 2 x 10^4 cells per 96 well plate. Sixteen hours later, cells were infected with WNV at a MOI of 5. Twenty-four hours later, cells were harvested and fixed and permeabilized using Foxp3/Transcription Factor Staining Buffer set. Subsequently, cells were incubated with rabbit anti-c-Myc (71D10; Cell Signaling) antibody or humanized E16 (68), a WNV E protein specific monoclonal antibody. After washing cells, AlexaFluro647-conjugated anti-rabbit-IgG (A-21245 Invitrogen) and AlexaFluor 568-conjugated anti-human IgG (A-21090 Invitrogen) secondary antibodies were added. Cells were analyzed on a BD LSRII flow cytometer array using FlowJo software.

Bone marrow chimera. 10^7 donor bone marrow cells from CD45.1 (B6.SJL) and CD45.2 (*Ifitm3*$^{-/-}$) mice were transferred adoptively by intravenous injection into 8 week-old recipient B6.SJL and *Ifitm3*$^{-/-}$ mice that had been irradiated with 900 cGγ. Mice were infected 8 weeks later with WNV. Tissues were harvested seven days after infection for viral burden and cellular immune response analysis as described above.

Statistical Analysis. Data was analyzed using Prism Software (GraphPad4, San Diego, CA). Kaplan-Meier survival curves were analyzed by the log rank test. A one-way or two-way ANOVA was used to determine statistically significant differences for *in vitro* viral growth experiments. The Mann-Whitney test was used to analyze differences in viral burden, cell numbers, and antibody titers. A one-way ANOVA with a multiple comparison correction was used to analyze difference in viral burden, cell numbers, and antibody titers for bone marrow chimera experiments.

RESULTS

Ifitm3 restricts WNV infection and pathogenesis in mice. IFITM3 is an ISG that has been reported to restrict infection of several flaviviruses in cell culture, including WNV and DENV (15, 19, 21–23, 69–71). To determine the role of Ifitm3 in restricting pathogenesis of a flavivirus *in vivo*, we inoculated 8 to 9 week-old WT and congenic *Ifitm3*$^{-/-}$ C57BL/6 mice via a subcutaneous route with 10^2 FFU of a pathogenic strain of WNV (New York 1999). *Ifitm3*$^{-/-}$ mice were more vulnerable to WNV infection than WT mice, as a greater percentage (90% versus 40% lethality, $P < 0.001$) succumbed to disease (**Fig 1A**). The mean time to death of *Ifitm3*$^{-/-}$ compared to WT mice was shorter (10.6 versus 11.8 days, $P < 0.05$), which is consistent with an accelerated disease course. One to two days before death, WT and *Ifitm3*$^{-/-}$ mice that ultimately would die similarly exhibited fur ruffling, hunched posture, and diminished movement. Within one day of death some of these animals developed clinical evidence of hind limb paralysis.

Ifitm3 limits WNV infection in different tissues. To begin to determine how an absence of Ifitm3 results in enhanced WNV pathogenesis, we measured viral burden in the serum, spleen, kidney, draining lymph nodes, brain, and spinal cord at days 2, 4, 6, and 8 post infection after subcutaneous infection.

Relatively small, yet statistically significant differences in viral burden were observed in some peripheral organs. For example, viremia was equivalent at day 2 after WNV infection but higher at days 4 and 6 in *Ifitm3*$^{-/-}$ compared to WT mice (**Fig 1B**, $P < 0.01$). Increased viral titers also were detected in the draining lymph node (DLN) days 6 and 8 after infection (**Fig 1C**, $P < 0.05$). However, an increase in WNV infection was not detected in the spleen at any of the time points (**Fig 1D**, $P > 0.05$). Viral yield remained near the limit of detection in the kidney of *Ifitm3*$^{-/-}$ mice (data not shown); in WT mice, this organ is normally resistant to WNV infection, but becomes susceptible in the absence of an intact type I IFN signaling response (72, 73).

We next assessed the impact of Ifitm3 on viral replication in the brain and spinal cord, which are targets of WNV infection in mice and humans (74). Higher viral titers were observed in the brains of *Ifitm3*$^{-/-}$ compared to WT mice at day 6 after infection (**Fig 1E,** $P < 0.05$) and in the spinal cord of *Ifitm3*$^{-/-}$ mice on days 6 and 8 after infection (**Fig 1F,** $P < 0.05$). Overall, an absence of Ifitm3 resulted in enhanced viral replication in the CNS.

Ifitm3 does not directly restrict WNV in infection in the CNS. The higher WNV titers in the brain and spinal cord of *Ifitm3*$^{-/-}$ mice could reflect enhanced replication in peripheral organs and viremia, which results in increased seeding of CNS tissues. Alternatively, it could be due to intrinsic antiviral effects of Ifitm3 in cells of the CNS. Although Ifitm3 is expressed in neurons at baseline and after type I IFN induction (74), it remains unknown whether Ifitm3 has an antiviral role in neurons *in vivo*. To evaluate this question, WT and *Ifitm3*$^{-/-}$ mice were infected with 10^1 FFU of WNV directly into the cerebral cortex via an intracranial route, and viral burden in the cerebral cortex, white matter, brain stem, cerebellum, and spinal cord was measured on days 3 and 5 after infection. Notably, no difference in viral burden was detected in CNS tissues on day 3 or day 5 after infection (**Fig 2A-F**, $P > 0.05$). Because the virulent strain of New York strain of WNV can antagonize IFN responses (75, 76), we repeated intracranial infection studies with an attenuated strain (Madagascar 1978 (WNV-MAD)) that is more sensitive to type I IFN (77). Again, no significant difference in viral burden was observed in CNS tissues of WNV-MAD-infected WT and *Ifitm3*$^{-/-}$ mice (**Fig 2G-L**, $P > 0.05$). These data suggest that the increased CNS titers in *Ifitm3*$^{-/-}$ mice after subcutaneous WNV infection were not due to direct antiviral effects in neuronal cells.

T cell responses in *Ifitm3*$^{-/-}$ mice. A previous study reported reduced $CD8^+$ T cell numbers in *Ifitm3*$^{-/-}$ mice during acute IAV infection (43). Another study demonstrated that lung resident memory $CD8^+$ T cells with reduced Ifitm3 expression were vulnerable to IAV infection and lost selectively during a secondary challenge (45). As depressed antiviral $CD8^+$ T cell also

can facilitate enhanced replication of WNV in the CNS (62, 78, 79), we investigated whether an absence of Ifitm3 influenced the development of an adaptive immune response during infection.

At day 7 after WNV infection, splenocytes were harvested and the percentage and number of bulk $CD4^+$ and $CD8^+$ T cells and NS4B tetramer-specific $CD8^+$ T cells were determined. Although differences in T cell numbers were not detected at baseline in naïve mice, the number of $CD4^+$ T cells, $CD8^+$ T cells, and NS4B tetramer-specific CD8 T cells was decreased in *Ifitm3*$^{-/-}$ mice after WNV infection (**Fig 3A-F, and M**). To assess whether antigen-specific $CD8^+$ T cells showed qualitative defects in the absence of Ifitm3, splenocytes were from WNV-infected mice were stimulated *ex vivo* with an immunodominant WNV NS4B peptide and tested for cytokine production. However, equivalent percentages, numbers, and geometric mean fluorescence intensity of IFN-γ and TNF-α producing $CD8^+$ T cells were detected in WT and *Ifitm3*$^{-/-}$ mice (**Fig 3G-L and N**, $P > 0.05$).

A small decrease in the number of antigen-specific $CD8^+$ T cells in the periphery of *Ifitm3*$^{-/-}$ mice could impact the accumulation of these cells in the CNS and viral clearance. As such, we compared the number of immune cells in the brains of WT and *Ifitm3*$^{-/-}$ mice at day 8 after infection by flow cytometry. We did not observe differences in the numbers of activated microglia ($CD11b^{high}$ $CD45^{low}$) or macrophages ($CD11b^{high}$ $CD45^{high}$) (**Fig 4A-D and 4S**, $P > 0.05$) in brains of WNV-infected WT and *Ifitm3*$^{-/-}$ mice. Moreover, similar percentages and numbers of NS4B tetramer$^+$ and granzyme B^+ $CD8^+$ T cells were detected (**Fig 4E-L**, $P > 0.05$). Also, after *ex vivo* restimulation with the NS4B peptide, equivalent percentages and numbers of IFN-γ and TNF-α secreting $CD8^+$ T cells were measured from the brains of WT and *Ifitm3*$^{-/-}$ mice (**Fig 4M-R, and 4T**, $P > 0.05$). Thus, while a small decrease in $CD8^+$ T cell response in the periphery of WNV-infected *Ifitm3*$^{-/-}$ mice was observed, it did not appear to impact clearance of virus in the spleen (see **Fig 1C**) or accumulation of antigen-specific immune cells in the brain.

293 **B cell responses in *Ifitm3*$^{-/-}$ mice.** Antiviral antibody responses restrict dissemination of
294 WNV *in vivo* into the CNS (59, 80). As such, we determined whether Ifitm3 expression
295 modulated antiviral antibody responses. Whereas baseline numbers of CD19^{+} B cells were
296 similar in naïve mice, we observed a decrease in their number in the spleen in *Ifitm3*$^{-/-}$ mice at
297 day 7 after infection (**Fig 5A and B**). To assess the effect on antiviral antibody responses, we
298 analyzed serum from WT and *Ifitm3*$^{-/-}$ mice on day 8 after infection for binding to WNV E protein.
299 Although anti-WNV IgM titers were equivalent between WT and *Ifitm3*$^{-/-}$ mice (**Fig 5C,** $P > 0.05$)
300 the anti-WNV IgG response was greater in *Ifitm3*$^{-/-}$ mice at day 8 after infection (**Fig 5D**, $P <$
301 0.05), possibly due to the higher levels of virus in peripheral organs. To evaluate the functional
302 quality of anti-WNV antibody from WT and *Ifitm3*$^{-/-}$ mice, we assessed neutralizing activity. No
303 difference in inhibitory activity was detected in serum from WT and *Ifitm3*$^{-/-}$ mice at day 8 post
304 infection (**Fig 5E**; $P > 0.05$). These data suggest that while there might be small effects of Ifiitm3
305 on B cell responses, these do not translate into depressed antiviral antibody responses, and
306 thus likely do not contribute to the increased WNV infection observed in different organs in
307 *Ifitm3*$^{-/-}$ mice.

308 **Ifitm3 controls WNV infection in some primary cells**. To gain further insight in which
309 cells require Ifitm3 for optimal restriction of WNV infection, we compared multi-step growth
310 kinetics and effects of IFN-β treatment in different primary cells derived from WT and *Ifitm3*$^{-/-}$
311 mice including Mϕ, DCs, and fibroblasts (MEFs). Although we did not observe statistically
312 increased viral yields in unstimulated *Ifitm3*$^{-/-}$ Mϕ (**Fig 6A**), pretreatment of *ifitm3*$^{-/-}$ Mϕ with low
313 doses of IFN-β to stimulate ISG production did produce marginally higher levels virus (**Fig 6B-**
314 **C**). In comparison, unstimulated or IFN-β-treated *Ifitm3*$^{-/-}$ DC did not support statistically
315 increased WNV infection (**Fig 6D-F**). However, multi-step growth analysis demonstrated
316 increased WNV yield in the supernatants of *Ifitm3*$^{-/-}$ compared to WT MEFs (**Fig 6G,** $P < 0.05$)
317 and this difference was amplified under conditions of IFN-β pre-treatment (**Fig 6H,** $P < 0.05$).

318 Single-step growth kinetic analysis failed to demonstrate increased WNV yield of unstimulated
319 *ifitm3*$^{-/-}$ MEFs (**Fig 6I**, P>0.05) although pretreatment with IFN-β did show an effect (**Fig 6J**, P
320 <0.05). Thus, Ifitm3 restricts WNV infection in some cell types although its expression must be
321 induced to observe this phenotype.

322 To confirm that the increased permissiveness of *Ifitm3*$^{-/-}$ MEF for WNV was due to the
323 loss of *Ifitm3*, we trans-complemented cells with a c-Myc tagged form of Ifitm3 (c-Myc-Ifitm3)
324 and compared this to a control c-Myc tagged form of Firefly luciferase (c-Myc-FLUC) (**Fig 6K-**
325 **M**). Lentiviral-mediated expression of c-Myc tagged Ifitm3 first was validated by Western
326 blotting (**Fig 6K**). Untransduced and c-Myc-FLUC transduced *Ifitm3*$^{-/-}$ and *Ifitm12356*$^{-/-}$ (locus
327 deletion) MEFs sustained higher WNV infection as judged by viral antigen staining and flow
328 cytometry when compared to the comparable Ifitm3-sufficient WT MEFs (3 to 4-fold, $P < 0.05$).
329 However, ectopic expression of c-Myc-Ifitm3 reduced WNV infection in WT, *Ifitm3*$^{-/-}$ (13-fold, $P <$
330 0.01) and *Ifitm12356*$^{-/-}$ (21-fold, $P < 0.001$) compared to expression of FLUC in these cells.
331 These data suggest that the relative susceptibility *Ifitm3*$^{-/-}$ and *Ifitm12356*$^{-/-}$ MEFs to WNV
332 infection is due largely to the loss of expression of Ifitm3, and that Ifitm3 can function as an
333 antiviral molecule in the absence of expression of Ifitm1, Ifitm2, Ifitm5, and Ifitm6.

334 ***Ifitm3 expression on radioresistant and radiosensitive cells restricts WNV***
335 ***infection.*** Our data in primary cells suggested that Ifitm3 might have antiviral effects in cells of
336 different lineages. To assess the relative importance of Ifitm3 in different cellular compartments
337 *in vivo*, we generated reciprocal bone marrow chimera using congenic CD45.1^{+} (WT) and
338 CD45.2^{+} (*Ifitm3*$^{-/-}$) donor and recipient mice, and viral burden was measured at 7 days after
339 infection (**Fig 7A-B**). Due to the process of irradiation and reconstitution, the chimeric mice
340 necessarily were infected at an older age, 16 weeks, compared to the other studies (see **Fig 1**).
341 Bone marrow chimeras with *Ifitm3*$^{-/-}$ or WT radio-resistant non-hematopoietic cells (WT→*Ifitm3*$^{-/-}$
342 or *Ifitm3*$^{-/-}$→WT) had equivalent levels of virus in serum, draining lymph node and spinal cord
343 (**Fig 7C-F**) at day 7 after infection compared to WT mice (WT→WT), whereas the *Ifitm3*$^{-/-}$ mice

(*Ifitm3*$^{-/-}$→*Ifitm3*$^{-/-}$) sustained higher titers in the brain (**Fig 7E**, $P < 0.05$), as seen with the direct gene deletions (see **Fig 1**). Analysis of the adaptive immune response revealed minor differences in the chimeric mice. The percentage of CD19^{+} B cells was higher in *Ifitm3*$^{-/-}$→*Ifitm3*$^{-/-}$ mice (**Fig 7G**), but no difference in the absolute number of CD19^{+} B cells was observed (**Fig 7H**). CD4^{+} T cell numbers and percentages in the spleen also were similar (**Fig 7I-J**). The percentage of CD8^{+} T cells was reduced in *Ifitm3*$^{-/-}$→WT and *Ifitm3*$^{-/-}$→*Ifitm3*$^{-/-}$ mice (**Fig 7K**), but this did not affect the total number of CD8^{+} T cells or the number or percentage of NS4B tetramer^{+} CD8^{+} T cells (**Fig 7L-N**). Thus, Ifitm3 expression in both radioresistant and radiosensitive cell compartments contributes to the control of WNV infection, and only when there is a lack of Ifitm3 in both compartments is the phenotype of enhanced infection in the CNS revealed.

DISCUSSION

Based primarily on studies in cell culture, the ISG IFITM3 has been suggested to have antiviral activity against a variety of viral pathogens, including flaviviruses (16–27). A demonstrable antiviral role for IFITM3/Ifitm3 *in vivo* has been established previously only for IAV and RSV (3, 43, 45, 46). We explored the function of Ifitm3 in restricting WNV pathogenesis in mice. Survival analysis revealed that *Ifitm3*$^{-/-}$ mice were more vulnerable to lethal WNV infection. This enhanced susceptibility was associated with increased viral infection in both peripheral and CNS tissues. Our culture studies with primary cells confirm an antiviral role of IFITM3 against WNV and extend these findings to a physiologically relevant *in vivo* system.

Several studies have examined the interaction between IFITM proteins and *Flaviviridae* members in cell culture (15, 19, 23, 69–71). DENV, WNV, YFV, and recently ZIKV were shown to be susceptible to IFITM-mediated antiviral restriction with IFITM3 being the most potent antiviral IFITM protein in cell culture (15, 71, 81). Mechanism of action studies demonstrated that IFITM3 had no significant effect of WNV RNA replication (19). Rather, flavivirus infection likely is inhibited by IFITM3 at the fusion step in the late endosome, analogous to its antiviral actions on IAV (33, 38, 39). Other work has shown that IFITM1, IFITM2, and IFITM3 all can restrict DENV infection including under conditions of antibody dependent enhancement (23). Our trans-complementation experiments in *Ifitm12356*$^{-/-}$ MEFs extend these findings by showing that Ifitm3 can inhibit infection of WNV independently of expression of Ifitm1, Ifitm2, Ifitm5, and Ifitm6. This data argues strongly against an essential role for heteromeric complexes of different IFITM proteins in the antiviral activity of IFITM3 (70, 82).

Few studies have examined the function of IFITM3 *in vivo*. Increased lethality of *Ifitm3*$^{-/-}$ mice was observed after challenge with IAV (43), and this was associated with increased viral titers in the lung, increased lung pathology, and lymphopenia compared to WT mice. An additional study observed that *Ifitm3*$^{-/-}$ and *Ifitm12356*$^{-/-}$ mice were equally susceptible to IAV suggesting that Ifitm3 may be the primary IFITM restriction (3). Of note, we were unable to study

382 WNV infection in *Ifitm12356*$^{-/-}$ mice, as virtually all of these animals were stillborn when crossed
383 onto a pure C57BL/6J background (M. J. Gorman and M. S. Diamond, unpublished
384 observations), which is consistent with the original description of several IFITM proteins having
385 a role in germ cell development (57, 83–85). *Ifitm3*$^{-/-}$ also were susceptible to another respiratory
386 virus, RSV, with increased viral titers in the lung after infection (46). Ifitm3, however, does not
387 restrict all pathogens, as *Ifitm3*$^{-/-}$ mice were not more susceptible to *Salmonella typhimurium*,
388 *Citrobacter rodentium, Mycobacterium tuberculosis* or *Plasmodium berghei* (46).

389 Prior studies have demonstrated Ifitm3 expression throughout the lung, spleen, lymph
390 node, liver, and intestine suggesting that this protein may have broad antiviral functions in many
391 tissues (3, 46). One of these functions may be the protection of immune cells such as CD8^{+}
392 resident memory T cells or dendritic cells, as increased IAV infection and reduced survival were
393 observed in Ifitm3-deficient T cells and dendritic cells (45, 86). Our studies demonstrate that
394 neurotropic viruses also are restricted by Ifitm3 *in vivo*, although this phenotype appeared
395 largely independent of a cell-intrinsic antiviral effect in the CNS. Our data is more consistent
396 with a dominant antiviral effect of Ifitm3 in cells of peripheral organs, which then limits viremia
397 and seeding of neurons in the brain and spinal cord. Our bone marrow chimera experiments
398 suggest that Ifitm3 expression on both radioresistant and radiosensitive cells contributes to the
399 control of WNV infection and pathogenesis *in vivo*. Definitive identification of the cells types *in*
400 *vivo* that require Ifitm3 for antiviral protection await the generation of conditional gene deletion
401 mice.

402 Similar to previously reported results, we discovered several adaptive immune
403 deficiencies during viral infection. IAV challenge models had demonstrated that *Ifitm3*$^{-/-}$ mice
404 had reduced CD4^{+} T cells and CD8^{+} T cell response in the lung during infection (43, 45). Our
405 data demonstrated a similar phenotype, with CD4^{+} T cells, CD8^{+} T cells, and CD19^{+} B cells
406 being reduced in the spleen during WNV infection. Despite this, antibody responses and CNS
407 infiltration by antigen-specific CD8^{+} T cells showed little defect in WNV-infected *Ifitm3*$^{-/-}$ mice.

Our bone marrow chimera experiments demonstrated that while the radiosensitive cells of the adaptive immune response may be important, they are not the dominant cell type leading to increased CNS viral burden.

IFITM3 is one of several ISGs that restrict WNV *in vivo* in mice. Antiviral functions against WNV have been documented for protein kinase R (PKR), RNAse L, Ifit2, Ifit27l2a, and viperin (49–52). Ifit2, Ifi27l2a, and viperin had antiviral functions that were limited largely to neurons in the CNS. Our data suggests that the dominant antiviral function of Ifitm3 likely occurs before WNV reaches the brain. Individual ISGs appear to have compartmentalized functions, and restrict WNV infection in a tissue-specific manner. The basis of this remains uncertain but could be determined by relative expression or interaction with partner proteins that are differentially expressed. Moreover, despite a highly intricate IFN-dependent signaling cascade in which hundreds of ISGs are induced in a single cell, deletion of single effector genes still can impact control of viral infection and disease outcome.

In summary, our study has demonstrated that Ifitm3 has an important antiviral function *in vivo* against WNV. As IFITM3 is one of several IFITM family members, which differ in their cellular localization, expression, and range of viral restriction, additional work is needed to determine whether other IFITM proteins have analogous antiviral functions *in vivo*.

426 **ACKNOWLEDGEMENTS**

427 National Institutes of Health grants U19 AI083019, U19 AI106772, R01 AI104972, and
428 R01 AI104002 supported this study. We would like to thank Tiffany Lucas and Amelia Pinto for
429 experimental advice and help with flow cytometry analysis. Experimental support for the speed
430 congenic backcrossing was provided by the Washington University Facility of the Rheumatic
431 Diseases Core Center. Research reported in this publication was supported by the National
432 Institute of Arthritis and Musculoskeletal and Skin Diseases, part of the National Institutes of
433 Health, under Award Number P30AR048335.

434

435 **REFERENCES**

436 1. **Hickford DE**, **Frankenberg SR**, **Shaw G**, **Renfree MB**. 2012. Evolution of vertebrate
437 interferon inducible transmembrane proteins. BMC Genomics **13**:155.
438 2. **Zhang Z**, **Liu J**, **Li M**, **Yang H**, **Zhang C**. 2012. Evolutionary dynamics of the interferon-
439 induced transmembrane gene family in vertebrates. PLoS One **7**:e49265.
440 3. **Bailey CC**, **Huang I-C**, **Kam C**, **Farzan M**. 2012. Ifitm3 limits the severity of acute
441 influenza in mice. PLoS Pathog. **8**:e1002909.
442 4. **Zhao X**, **Guo F**, **Liu F**, **Cuconati A**, **Chang J**, **Block TM**, **Guo J-T**. 2014. Interferon
443 induction of IFITM proteins promotes infection by human coronavirus OC43. Proc. Natl.
444 Acad. Sci. U. S. A. **111**:6756–61.
445 5. **Evans SS**, **Lee DB**, **Han T**, **Tomasi TB**, **Evans RL**. 1990. Monoclonal antibody to the
446 interferon-inducible protein Leu-13 triggers aggregation and inhibits proliferation of
447 leukemic B cells. Blood **76**:2583–93.
448 6. **Takahashi S**, **Doss C**, **Levy S**, **Levy R**. 1990. TAPA-1, the target of an antiproliferative
449 antibody, is associated on the cell surface with the Leu-13 antigen. J. Immunol.
450 **145**:2207–13.
451 7. **Bradbury LE**, **Goldmacher VS**, **Tedder TF**. 1993. The CD19 signal transduction
452 complex of B lymphocytes. Deletion of the CD19 cytoplasmic domain alters signal
453 transduction but not complex formation with TAPA-1 and Leu 13. J. Immunol. **151**:2915–
454 27.
455 8. **Frey M**, **Appenheimer MM**, **Evans SS**. 1997. Tyrosine kinase-dependent regulation of L-
456 selectin expression through the Leu-13 signal transduction molecule: evidence for a
457 protein kinase C-independent mechanism of L-selectin shedding. J. Immunol. **158**:5424–
458 34.
459 9. **Tanaka SS**, **Matsui Y**. 2002. Developmentally regulated expression of mil-1 and mil-2,
460 mouse interferon-induced transmembrane protein like genes, during formation and

differentiation of primordial germ cells. Mech. Dev. **119 Suppl** :S261–7.

10. **Zucchi I**, **Prinetti a**, **Scotti M**, **Valsecchi V**, **Valaperta R**, **Mento E**, **Reinbold R**, **Vezzoni P**, **Sonnino S**, **Albertini a**, **Dulbecco R**. 2004. Association of rat8 with Fyn protein kinase via lipid rafts is required for rat mammary cell differentiation in vitro. Proc. Natl. Acad. Sci. U. S. A. **101**:1880–5.

11. **Martensen PM**, **Justesen J**. 2004. Small ISGs coming forward. J. Interferon Cytokine Res. **24**:1–19.

12. **Yang G**, **Xu Y**, **Chen X**, **Hu G**. 2007. IFITM1 plays an essential role in the antiproliferative action of interferon-gamma. Oncogene **26**:594–603.

13. **Daniel-Carmi V**, **Makovitzki-Avraham E**, **Reuven E-M**, **Goldstein I**, **Zilkha N**, **Rotter V**, **Tzehoval E**, **Eisenbach L**. 2009. The human 1-8D gene (IFITM2) is a novel p53 independent pro-apoptotic gene. Int. J. Cancer **125**:2810–9.

14. **Alber D**, **Staeheli P**. 1996. Partial inhibition of vesicular stomatitis virus by the interferon-induced human 9-27 protein. J. Interferon Cytokine Res. **16**:375–80.

15. **Brass AL**, **Huang I-C**, **Benita Y**, **John SP**, **Krishnan MN**, **Feeley EM**, **Ryan BJ**, **Weyer JL**, **van der Weyden L**, **Fikrig E**, **Adams DJ**, **Xavier RJ**, **Farzan M**, **Elledge SJ**. 2009. The IFITM proteins mediate cellular resistance to influenza A H1N1 virus, West Nile virus, and dengue virus. Cell **139**:1243–54.

16. **Diamond MS**, **Farzan M**. 2012. The broad-spectrum antiviral functions of IFIT and IFITM proteins. Nat. Rev. Immunol. **13**:46–57.

17. **Bailey CC**, **Zhong G**, **Huang I**, **Farzan M**. 2014. IFITM-Family Proteins: The Cell's First Line of Antiviral Defense. Annu. Rev. Virol. **1**:261–283.

18. **Weidner JM**, **Jiang D**, **Pan X-B**, **Chang J**, **Block TM**, **Guo J-T**. 2010. Interferon-induced cell membrane proteins, IFITM3 and tetherin, inhibit vesicular stomatitis virus infection via distinct mechanisms. J. Virol. **84**:12646–57.

19. **Jiang D**, **Weidner JM**, **Qing M**, **Pan X-B**, **Guo H**, **Xu C**, **Zhang X**, **Birk A**, **Chang J**, **Shi**

P-Y, **Block TM**, **Guo J-T**. 2010. Identification of five interferon-induced cellular proteins that inhibit west nile virus and dengue virus infections. J. Virol. **84**:8332–41.

20. **Huang I-C**, **Bailey CC**, **Weyer JL**, **Radoshitzky SR**, **Becker MM**, **Chiang JJ**, **Brass AL**, **Ahmed A a**, **Chi X**, **Dong L**, **Longobardi LE**, **Boltz D**, **Kuhn JH**, **Elledge SJ**, **Bavari S**, **Denison MR**, **Choe H**, **Farzan M**. 2011. Distinct patterns of IFITM-mediated restriction of filoviruses, SARS coronavirus, and influenza A virus. PLoS Pathog. **7**:e1001258.

21. **Raychoudhuri A**, **Shrivastava S**, **Steele R**, **Kim H**, **Ray R**, **Ray RB**. 2011. ISG56 and IFITM1 proteins inhibit hepatitis C virus replication. J. Virol. **85**:12881–9.

22. **Wilkins C**, **Woodward J**, **Lau DT-Y**, **Barnes A**, **Joyce M**, **McFarlane N**, **Tyrrell DL**, **Gale M**. 2012. IFITM1 is a tight junction protein that inhibits hepatitis C virus entry. Hepatology **024563**:1–9.

23. **Chan YK**, **Huang I-C**, **Farzan M**. 2012. IFITM proteins restrict antibody-dependent enhancement of dengue virus infection. PLoS One **7**:e34508.

24. **Mudhasani R**, **Tran JP**, **Retterer C**, **Radoshitzky SR**, **Kota KP**, **Altamura L a**, **Smith JM**, **Packard BZ**, **Kuhn JH**, **Costantino J**, **Garrison AR**, **Schmaljohn CS**, **Huang I-C**, **Farzan M**, **Bavari S**. 2013. IFITM-2 and IFITM-3 but not IFITM-1 restrict Rift Valley fever virus. J. Virol. **87**:8451–64.

25. **Smith SE**, **Gibson MS**, **Wash RS**, **Ferrara F**, **Wright E**, **Temperton N**, **Kellam P**, **Fife M**. 2013. Chicken interferon-inducible transmembrane protein 3 restricts influenza viruses and lyssaviruses in vitro. J. Virol. **87**:12957–66.

26. **Zhang W**, **Zhang L**, **Zan Y**, **Du N**, **Yang Y**, **Tien P**. 2015. Human respiratory syncytial virus infection is inhibited by IFN-induced transmembrane proteins. J. Gen. Virol. **96**:170–82.

27. **Qian J**, **Duff Y Le**, **Wang Y**, **Pan Q**, **Ding S**, **Zheng Y-M**, **Liu S-L**, **Liang C**. 2014. Primate lentiviruses are differentially inhibited by interferon-induced transmembrane proteins. Virology **474C**:10–18.

28. **Weston S**, **Czieso S**, **White IJ**, **Smith SE**, **Wash RS**, **Diaz-Soria C**, **Kellam P**, **Marsh M**. 2016. Alphavirus restriction by IFITM proteins. Traffic.

29. **Warren CJ**, **Griffin LM**, **Little AS**, **Huang I-C**, **Farzan M**, **Pyeon D**. 2014. The antiviral restriction factors IFITM1, 2 and 3 do not inhibit infection of human papillomavirus, cytomegalovirus and adenovirus. PLoS One **9**:e96579.

30. **Chen YX**, **Welte K**, **Gebhard DH**, **Evans RL**. 1984. Induction of T cell aggregation by antibody to a 16kd human leukocyte surface antigen. J. Immunol. **133**:2496–501.

31. **Yount JS**, **Karssemeijer R a**, **Hang HC**. 2012. S-palmitoylation and ubiquitination differentially regulate interferon-induced transmembrane protein 3 (IFITM3)-mediated resistance to influenza virus. J. Biol. Chem. **287**:19631–41.

32. **Jia R**, **Pan Q**, **Ding S**, **Rong L**, **Liu S-L**, **Geng Y**, **Qiao W**, **Liang C**. 2012. The N-terminal region of IFITM3 modulates its antiviral activity by regulating IFITM3 cellular localization. J. Virol. **86**:13697–707.

33. **Li K**, **Markosyan RM**, **Zheng Y-M**, **Golfetto O**, **Bungart B**, **Li M**, **Ding S**, **He Y**, **Liang C**, **Lee JC**, **Gratton E**, **Cohen FS**, **Liu S-L**. 2013. IFITM Proteins Restrict Viral Membrane Hemifusion. PLoS Pathog. **9**:e1003124.

34. **Hach JC**, **McMichael T**, **Chesarino NM**, **Yount JS**. 2013. Palmitoylation on conserved and nonconserved cysteines of murine IFITM1 regulates its stability and anti-influenza A virus activity. J. Virol. **87**:9923–7.

35. **Bailey CC**, **Kondur HR**, **Huang I-C**, **Farzan M**. 2013. Interferon-induced transmembrane protein 3 is a type II transmembrane protein. J. Biol. Chem. **288**:32184–93.

36. **Weston S**, **Czieso S**, **White IJ**, **Smith SE**, **Kellam P**, **Marsh M**. 2014. A membrane topology model for human interferon inducible transmembrane protein 1. PLoS One **9**:e104341.

37. **Ling S**, **Zhang C**, **Wang W**, **Cai X**, **Yu L**, **Wu F**, **Zhang L**, **Tian C**. 2016. Combined approaches of EPR and NMR illustrate only one transmembrane helix in the human

IFITM3. Sci. Rep. **6**:24029.

38. **Desai TM**, **Marin M**, **Chin CR**, **Savidis G**, **Brass AL**, **Melikyan GB**. 2014. IFITM3 Restricts Influenza A Virus Entry by Blocking the Formation of Fusion Pores following Virus-Endosome Hemifusion. PLoS Pathog. **10**:e1004048.

39. **Feeley EM**, **Sims JS**, **John SP**, **Chin CR**, **Pertel T**, **Chen L-M**, **Gaiha GD**, **Ryan BJ**, **Donis RO**, **Elledge SJ**, **Brass AL**. 2011. IFITM3 inhibits influenza A virus infection by preventing cytosolic entry. PLoS Pathog. **7**:e1002337.

40. **Amini-bavil-olyaee S**, **Choi YJ**, **Lee JH**, **Shi M**, **Huang I**, **Farzan M**. 2013. Article The Antiviral Effector IFITM3 Disrupts Intracellular Cholesterol Homeostasis to Block Viral Entry. Cell Host Microbe **13**:452–464.

41. **Compton AA**, **Bruel T**, **Porrot F**, **Mallet A**, **Sachse M**, **Euvrard M**, **Liang C**, **Casartelli N**, **Schwartz O**. 2014. IFITM proteins incorporated into HIV-1 virions impair viral fusion and spread. Cell Host Microbe **16**:736–47.

42. **Tartour K**, **Appourchaux R**, **Gaillard J**, **Nguyen X-N**, **Durand S**, **Turpin J**, **Beaumont E**, **Roch E**, **Berger G**, **Mahieux R**, **Brand D**, **Roingeard P**, **Cimarelli A**. 2014. IFITM proteins are incorporated onto HIV-1 virion particles and negatively imprint their infectivity. Retrovirology **11**:103.

43. **Everitt AR**, **Clare S**, **Pertel T**, **John SP**, **Wash RS**, **Smith SE**, **Chin CR**, **Feeley EM**, **Sims JS**, **Adams DJ**, **Wise HM**, **Kane L**, **Goulding D**, **Digard P**, **Anttila V**, **Baillie JK**, **Walsh TS**, **Hume D a**, **Palotie A**, **Xue Y**, **Colonna V**, **Tyler-Smith C**, **Dunning J**, **Gordon SB**, **Smyth RL**, **Openshaw PJ**, **Dougan G**, **Brass AL**, **Kellam P**. 2012. IFITM3 restricts the morbidity and mortality associated with influenza. Nature **484**:519–23.

44. **Jia R**, **Xu F**, **Qian J**, **Yao Y**, **Miao C**, **Zheng Y-M**, **Liu S-L**, **Guo F**, **Geng Y**, **Qiao W**, **Liang C**. 2014. Identification of an endocytic signal essential for the antiviral action of IFITM3. Cell. Microbiol. **16**:1080–93.

45. **Wakim LM**, **Gupta N**, **Mintern JD**, **Villadangos J a**. 2013. Enhanced survival of lung

tissue-resident memory CD8$^+$ T cells during infection with influenza virus due to selective expression of IFITM3. Nat. Immunol. **14**:238–45.

46. **Everitt AR**, **Clare S**, **McDonald JU**, **Kane L**, **Harcourt K**, **Ahras M**, **Lall A**, **Hale C**, **Rodgers A**, **Young DB**, **Haque A**, **Billker O**, **Tregoning JS**, **Dougan G**, **Kellam P**. 2013. Defining the range of pathogens susceptible to ifitm3 restriction using a knockout mouse model. PLoS One **8**:e80723.

47. **Armah HB**, **Wang G**, **Omalu BI**, **Tesh RB**, **Gyure K a**, **Chute DJ**, **Smith RD**, **Dulai P**, **Vinters H V**, **Kleinschmidt-DeMasters BK**, **Wiley C a**. 2007. Systemic distribution of West Nile virus infection: postmortem immunohistochemical study of six cases. Brain Pathol. **17**:354–362.

48. **Omalu BI**, **Shakir AA**, **Wang G**, **Lipkin WI**, **Wiley CA**. 2003. Fatal fulminant pan-meningo-polioencephalitis due to West Nile virus. Brain Pathol. **13**:465–72.

49. **Samuel M a**, **Whitby K**, **Keller BC**, **Marri A**, **Barchet W**, **Williams BRG**, **Silverman RH**, **Gale M**, **Diamond MS**. 2006. PKR and RNase L contribute to protection against lethal West Nile Virus infection by controlling early viral spread in the periphery and replication in neurons. J. Virol. **80**:7009–19.

50. **Szretter KJ**, **Brien JD**, **Thackray LB**, **Virgin HW**, **Cresswell P**, **Diamond MS**. 2011. The interferon-inducible gene viperin restricts West Nile virus pathogenesis. J. Virol. **85**:11557–66.

51. **Cho H**, **Shrestha B**, **Sen GC**, **Diamond MS**. 2013. A role for Ifit2 in restricting West Nile virus infection in the brain. J. Virol. **87**:8363–71.

52. **Lucas TM**, **Richner JM**, **Diamond MS**. 2016. The Interferon-Stimulated Gene Ifi27l2a Restricts West Nile Virus Infection and Pathogenesis in a Cell-Type- and Region-Specific Manner. J. Virol. **90**:2600–15.

53. **Lanciotti RS**, **Ebel GD**, **Deubel V**, **Kerst AJ**, **Murri S**, **Meyer R**, **Bowen M**, **McKinney N**, **Morrill WE**, **Crabtree MB**, **Kramer LD**, **Roehrig JT**. 2002. Complete genome

sequences and phylogenetic analysis of West Nile virus strains isolated from the United States, Europe, and the Middle East. Virology **298**:96–105.

54. **Ebel GD**, **Carricaburu J**, **Young D**, **Bernard K a**, **Kramer LD**. 2004. Genetic and phenotypic variation of West Nile virus in New York, 2000-2003. Am. J. Trop. Med. Hyg. **71**:493–500.

55. **Beasley DWC**, **Li L**, **Suderman MT**, **Barrett ADT**. 2002. Mouse neuroinvasive phenotype of West Nile virus strains varies depending upon virus genotype. Virology **296**:17–23.

56. **Brien JD**, **Lazear HM**, **Diamond MS**. 2013. Propagation, quantification, detection and Storage of West Nile Virus. Curr. Protoc. Microbiol. **31**:15D3.1–15D3.18.

57. **Lange UC**, **Adams DJ**, **Lee C**, **Barton S**, **Schneider R**, **Bradley A**, **Surani MA**. 2008. Normal germ line establishment in mice carrying a deletion of the Ifitm/Fragilis gene family cluster. Mol. Cell. Biol. **28**:4688–96.

58. **Szretter KJ**, **Daffis S**, **Patel J**, **Suthar MS**, **Klein RS**, **Gale M**, **Diamond MS**. 2010. The Innate Immune Adaptor Molecule MyD88 Restricts West Nile Virus Replication and Spread in Neurons of the Central Nervous System. J. Virol. **84**:12125–12138.

59. **Diamond MS**, **Shrestha B**, **Marri A**, **Mahan D**, **Engle M**. 2003. B Cells and Antibody Play Critical Roles in the Immediate Defense of Disseminated Infection by West Nile Encephalitis Virus B Cells and Antibody Play Critical Roles in the Immediate Defense of Disseminated Infection by West Nile Encephalitis Virus. J. Virol. **77**:2578–2586.

60. **Lanciotti RS**, **Kerst a. J**, **Nasci RS**, **Godsey MS**, **Mitchell CJ**, **Savage HM**, **Komar N**, **Panella N a.**, **Allen BC**, **Volpe KE**, **Davis BS**, **Roehrig JT**. 2000. Rapid detection of West Nile virus from human clinical specimens, field-collected mosquitoes, and avian samples by a TaqMan reverse transcriptase-PCR assay. J. Clin. Microbiol. **38**:4066–4071.

61. **Mehlhop E**, **Diamond MS**. 2006. Protective immune responses against West Nile virus

are primed by distinct complement activation pathways. J. Exp. Med. **203**:1371–1381.

62. **Purtha WE**, **Myers N**, **Mitaksov V**, **Sitati E**, **Connolly J**, **Fremont DH**, **Hansen TH**, **Diamond MS**. 2007. Antigen-specific cytotoxic T lymphocytes protect against lethal West Nile virus encephalitis. Eur. J. Immunol. **37**:1845–54.

63. **Szretter KJ**, **Samuel MA**, **Gilfillan S**, **Fuchs A**, **Colonna M**, **Diamond MS**. 2009. The Immune Adaptor Molecule SARM Modulates Tumor Necrosis Factor Alpha Production and Microglia Activation in the Brainstem and Restricts West Nile Virus Pathogenesis. J. Virol. **83**:9329–9338.

64. **Lazear HM**, **Pinto AK**, **Vogt MR**, **Gale M**, **Diamond MS**. 2011. Beta interferon controls West Nile virus infection and pathogenesis in mice. J. Virol. **85**:7186–7194.

65. **Dora S**, **Schwarz C**, **Baack M**, **Graessmann A**, **Knippers R**. 1989. Analysis of a large-T-antigen variant expressed in simian virus 40-transformed mouse cell line mKS-A. J Virol **63**:2820–2828.

66. **Araki T**, **Sasaki Y**, **Milbrandt J**. 2004. Increased nuclear NAD biosynthesis and SIRT1 activation prevent axonal degeneration. Science **305**:1010–3.

67. **Dull T**, **Zufferey R**, **Kelly M**, **Mandel RJ**, **Nguyen M**, **Trono D**, **Naldini L**. 1998. A third-generation lentivirus vector with a conditional packaging system. J. Virol. **72**:8463–71.

68. **Oliphant T**, **Engle M**, **Nybakken GE**, **Doane C**, **Johnson S**, **Huang L**, **Gorlatov S**, **Mehlhop E**, **Marri A**, **Chung KM**, **Ebel GD**, **Kramer LD**, **Fremont DH**, **Diamond MS**. 2005. Development of a humanized monoclonal antibody with therapeutic potential against West Nile virus. Nat. Med. **11**:522–30.

69. **Zhu X**, **He Z**, **Yuan J**, **Wen W**, **Huang X**, **Hu Y**, **Lin C**, **Pan J**, **Li R**, **Deng H**, **Liao S**, **Zhou R**, **Wu J**, **Li J**, **Li M**. 2015. IFITM3-containing exosome as a novel mediator for anti-viral response in dengue virus infection. Cell. Microbiol. **17**:105–18.

70. **John SP**, **Chin CR**, **Perreira J**, **Feeley EM**, **Aker A**, **Savidis G**, **Smith SE**, **Elia AEH**, **Everitt AR**, **Vora M**, **Pertel T**, **Elledge SJ**, **Kellam P**, **Brass AL**. 2013. The CD225

643 Domain of IFITM3 is Required for both IFITM Protein Association and Inhibition of
644 Influenza A Virus and Dengue Virus Replication. J. Virol. **87**:7837–7852.
645 71. **Schoggins JW**, **Wilson SJ**, **Panis M**, **Murphy MY**, **Jones CT**, **Bieniasz P**, **Rice CM**.
646 2011. A diverse range of gene products are effectors of the type I interferon antiviral
647 response. Nature **472**:481–5.
648 72. **Suthar MS**, **Ma DY**, **Thomas S**, **Lund JM**, **Zhang N**, **Daffis S**, **Rudensky AY**, **Bevan**
649 **MJ**, **Clark E a**, **Kaja M-K**, **Diamond MS**, **Gale M**. 2010. IPS-1 is essential for the control
650 of West Nile virus infection and immunity. PLoS Pathog. **6**:e1000757.
651 73. **Daffis S**, **Samuel M a.**, **Keller BC**, **Gale M**, **Diamond MS**. 2007. Cell-specific IRF-3
652 responses protect against West Nile virus infection by interferon-dependent and -
653 independent mechanisms. PLoS Pathog. **3**:1005–1015.
654 74. **Cho H**, **Proll SC**, **Szretter KJ**, **Katze MG**, **Gale M**, **Diamond MS**. 2013. Differential
655 innate immune response programs in neuronal subtypes determine susceptibility to
656 infection in the brain by positive-stranded RNA viruses. Nat. Med. **19**:458–64.
657 75. **Laurent-Rolle M**, **Boer EF**, **Lubick KJ**, **Wolfinbarger JB**, **Carmody AB**, **Rockx B**, **Liu**
658 **W**, **Ashour J**, **Shupert WL**, **Holbrook MR**, **Barrett AD**, **Mason PW**, **Bloom ME**, **García-**
659 **Sastre A**, **Khromykh A a**, **Best SM**. 2010. The NS5 protein of the virulent West Nile
660 virus NY99 strain is a potent antagonist of type I interferon-mediated JAK-STAT
661 signaling. J. Virol. **84**:3503–3515.
662 76. **Fredericksen BL**, **Gale M**. 2006. West Nile virus evades activation of interferon
663 regulatory factor 3 through RIG-I-dependent and -independent pathways without
664 antagonizing host defense signaling. J. Virol. **80**:2913–23.
665 77. **Keller BC**, **Fredericksen BL**, **Samuel M a**, **Mock RE**, **Mason PW**, **Diamond MS**, **Gale**
666 **M**. 2006. Resistance to alpha/beta interferon is a determinant of West Nile virus
667 replication fitness and virulence. J. Virol. **80**:9424–34.
668 78. **Brien JD**, **Uhrlaub JL**, **Nikolich-Zugich J**. 2007. Protective capacity and epitope

specificity of CD8(+) T cells responding to lethal West Nile virus infection. Eur. J. Immunol. **37**:1855–63.

79. **Shrestha B**, **Diamond MS**. 2004. Role of CD8 ϩ T Cells in Control of West Nile Virus Infection **78**:8312–8321.

80. **Diamond MS**, **Sitati EM**, **Friend LD**, **Higgs S**, **Shrestha B**, **Engle M**. 2003. A critical role for induced IgM in the protection against West Nile virus infection. J. Exp. Med. **198**:1853–62.

81. **Savidis G**, **Perreira JM**, **Portmann JM**, **Meraner P**, **Guo Z**, **Green S**, **Brass AL**. 2016. The IFITMs Inhibit Zika Virus Replication. Cell Rep. **15**:2323–30.

82. **Perreira JM**, **Chin CR**, **Feeley EM**, **Brass AL**. 2013. IFITMs restrict the replication of multiple pathogenic viruses. J. Mol. Biol. **425**:4937–55.

83. **Tanaka SS**, **Yamaguchi YL**, **Tsoi B**, **Lickert H**, **Tam PPL**. 2005. IFITM/Mil/fragilis family proteins IFITM1 and IFITM3 play distinct roles in mouse primordial germ cell homing and repulsion. Dev. Cell **9**:745–56.

84. **Lange UC**, **Saitou M**, **Western PS**, **Barton SC**, **Surani M a**. 2003. The fragilis interferon-inducible gene family of transmembrane proteins is associated with germ cell specification in mice. BMC Dev. Biol. **3**:1.

85. **Saitou M**, **Barton SC**, **Surani MA**. 2002. A molecular programme for the specification of germ cell fate in mice. Nature **418**:293–300.

86. **Infusini G**, **Smith JM**, **Yuan H**, **Pizzolla A**, **Ng WC**, **Londrigan SL**, **Haque A**, **Reading PC**, **Villadangos JA**, **Wakim LM**. 2015. Respiratory DC Use IFITM3 to Avoid Direct Viral Infection and Safeguard Virus-Specific CD8+ T Cell Priming. PLoS One **10**:e0143539.

693 **FIGURE LEGENDS**

694 **Figure 1. Survival and viral burden analysis of WT and *Ifitm3*$^{-/-}$ mice**. **A**. Eight to ten
695 week-old age-matched WT (*n* = 28) and *Ifitm3*$^{-/-}$ (*n* = 23) C57BL/6 mice were infected via
696 subcutaneous route with 10^2 FFU of WNV (New York 1999) and monitored for mortality for 21
697 days. Survival differences were analyzed by the log rank test ($P < 0.005$). **B to F**. WNV tissue
698 burden in WT and *Ifitm3*$^{-/-}$ mice after subcutaneous infection. WNV levels in serum (**B**), draining
699 lymph node (**C**), spleen (**D**), brain (**E**), and spinal cord (**F**) were measured by qRT-PCR (**B-C**) or
700 plaque assay (**D-F**). Solid lines represent the median viral titers, and dotted lines denote the
701 limit of detection of the assay. 2-3 mice were used per independent experiment and 5-7
702 independent experiments were performed. Asterisks indicate statistically significant differences
703 by the Mann-Whitney test (* $P < 0.05$, ** $P < 0.01$, *** $P < 0.001$).

704 **Figure 2. No difference in CNS viral burden via intracranial route of inoculation**.
705 Eight to ten week-old age-matched WT and *Ifitm3*$^{-/-}$ C57BL/6 mice were inoculated via an
706 intracranial route with 10^1 FFU of (**A-F**) WNV (New York 1999) or (**G-L**) WNV-MAD
707 (Madagascar 1978). Tissues were harvested at day 3 or day 5 after infection. WNV levels in
708 olfactory bulb (**A, G**), brain stem (**B, H**), cerebellum (**C, I**), cerebral cortex white matter (**D, J**),
709 cerebral cortex gray matter (**E, K**), and spinal cord (**F, L**) were measured by plaque assay. Solid
710 lines represent the median viral titers, and dotted lines denote the limit of detection of the assay.
711 2-3 mice were used per independent experiment, and 3-4 independent experiments were
712 performed. None of the comparisons were statistically different as determined by the Mann-
713 Whitney test (Panels **A-L**, $P > 0.05$).

714 **Figure 3. *Ifitm3*$^{-/-}$ mice have blunted T cell responses in the spleen after WNV**
715 **infection**. Immune responses were examined in the spleen after subcutaneous inoculation of
716 10^2 FFU of WNV (New York 1999). Spleens were harvested on day 7 (**A-H**) or 8 (**I-N**) after
717 infection. The percentage of live cells and total cell population of (**A-B**) $CD3^+$ $CD4^+$ T cells, (**C-D**)
718 $CD3^+$ $CD8^+$ T cells, (**E-F**) NS4B-specific $CD3^+$ $CD8^+$ T cells were measured. The percentage of

719 $CD8^+$ T cells and total numbers of $CD3^+$ $CD8^+$ T cells that expressed IFN-γ (**G-H**), TNF-α (**I-J**),
720 or TNF-α and IFN-γ (**K-L**) after *ex vivo* stimulation with NS4B peptide are indicated.
721 Representative flow cytometry plots of NS4B-specific $CD3^+$ $CD8^+$ T cells (**M**) and $CD3^+$ $CD8^+$
722 that express TNF-α and IFN-γ after peptide restimulation (**N**) are shown. 4-5 mice were used
723 per independent experiment, and 4 independent experiments were performed. Statistical
724 significance was determined by the Mann-Whitney test (* $P < 0.05$, ** $P < 0.01$).

725 **Figure 4. *Ifitm3*$^{-/-}$ mice have normal levels of immune cell populations in the brain**
726 **after WNV infection.** CNS immune responses were examined after subcutaneous inoculation
727 of of 10^2 FFU of WNV (New York 1999). Brains were harvested day 8 post infection. The
728 percentage and total number of (**A-B**) $CD11b^+$ $CD45^{lo}$ microglia, (**C-D**) $CD11b^+$ $CD45^{hi}$
729 macrophages, (**E-F**) $CD4^+$ T cells, (**G-H**) $CD8^+$ T cells, (**I-J**) $CD8^+$ granzyme B^+ T cells, and (**K-**
730 **L**) NS4B-specific $CD8^+$ T cells are shown. The percentage and total number of $CD8^+$ T cells that
731 expressed (**M-N**) IFN-γ, (**O-P**) TNF-α, or (**Q-R**) both IFN-γ and TNF-α after NS4B peptide
732 restimulation are shown. 3 mice were used per independent experiment and 3 independent
733 experiments were performed. None of the comparisons were statistically different as determined
734 by the Mann-Whitney test ($P > 0.05$).

735 **Figure 5. *Ifitm3*$^{-/-}$ mice have reduced B cell numbers but not reduced antiviral**
736 **antibody titers. A-B**. Spleens were harvested at day 7 after after subcutaneous inoculation of
737 WNV (New York 1999). (**A**) The percentage and (**B**) total cell numbers of B cells were
738 determined by flow cytometry. **C-E**. Serum was harvested at day 8 after infection. IgM and IgG
739 antibody titers (**C, D**) were determined using an ELISA against purified WNV E protein. Serum
740 neutralization activity (**E**) was evaluated using an focus reduction neutralization test, and data
741 was fitted by regression analysis to obtain EC50 values. 2-5 mice were used per independent
742 experiment, and 4 independent experiments were performed. Statistical significance was
743 determined by the Mann-Whitney test (* $P < 0.05$).

744 **Figure 6. WNV infection in Mϕ, DC, and MEFs.** Bone marrow derived Mϕ (**A-C**) and
745 DCs (**D-F**) were infected at a MOI of 0.01 with WNV (New York 1999) and MEFs (**G-J**) were
746 infected at an MOI of 5 or 0.01 with WNV (New York 1999). In some experiments, cells were
747 pretreated for 16 h with 0 0.1, 1, or 10 U/mL of IFN-β. Viral titers were determined by focus-
748 forming assays and reflects at least three independent experiments. **K-M**. Transformed WT,
749 *Ifitm12356*$^{-/-}$, or *Ifitm3*$^{-/-}$ MEFs were transduced with lentiviruses expressing a c-Myc tagged
750 Ifitm3 or Firefly luciferase (FLUC). Lentiviral-mediated expression of Ifitm3 was validated by
751 Western blotting and compared to endogenous Ifitm3 expression levels in WT MEFs pretreated
752 for 16 h with 10 U/mL of IFN-β (**K**). Transduced MEFs were infected with WNV (New York 1999)
753 at an MOI of 0.01 for 24 h. Cells were harvested and flow cytometry was used to detect
754 expression of c-Myc tagged proteins and WNV-infected cells. Representative flow cytometry
755 plots (**L**) and pooled data (**M**) are shown from at least 3 independent experiments performed in
756 duplicate. Statistical significance in this Figure was determined by a one-way (**M**) or two-way (**A-**
757 **J**) ANOVA (* $P < 0.05$, ** $P < 0.01$, *** $P < 0.001$).

758 **Figure 7. Ifitm3 has functions in both the hematopoietic and nonhematopoietic**
759 **cell compartments to restrict WNV infection.** (**A**) CD45.1$^+$ B6.SJL and CD45.2$^+$ *Ifitm3*$^{-/-}$ mice
760 were sublethally irradiated and reconstituted with either CD45.1$^+$ B6.SJL or CD45.2$^+$ *Ifitm3*$^{-/-}$
761 bone marrow (10^7 cells). Representative flow cytometry plots are shown of CD45.1 versus
762 CD45.2 for CD19$^+$ B cells and CD3$^+$ T cells after reconstitution (**B**). Sixteen week-old chimeric
763 mice were inoculated via subcutaneous route with 10^2 FFU of WNV (New York 1999) and
764 tissues were harvested at day 7 after infection. WNV levels in serum (**C**), draining lymph node
765 (**D**), brain (**E**), and spinal cord (**F**) were measured by qRT-PCR (**C-D**) or by infectious plaque
766 assay (**E-F**). Solid lines represent the median viral titers, and dotted lines denote the limit of
767 detection of the assay. Percentage and total cell numbers in the spleen of (**G-H**) CD19$^+$ B cells,
768 (**I-J**) CD3$^+$ CD4$^+$ T cells, (**K-L**) CD3$^+$ CD8$^+$ T cells, (**M-N**) NS4B-specific CD3$^+$ CD8$^+$ T cells. 2-4
769 animals were used per independent experiment, and 2 independent experiments were

performed. Asterisks indicate values that are statistically significant by a non-parametric (**C-F**) or (**H-N**) parametric ANOVA (* $P < 0.05$, ** $P < 0.01$, *** $P < 0.001$).

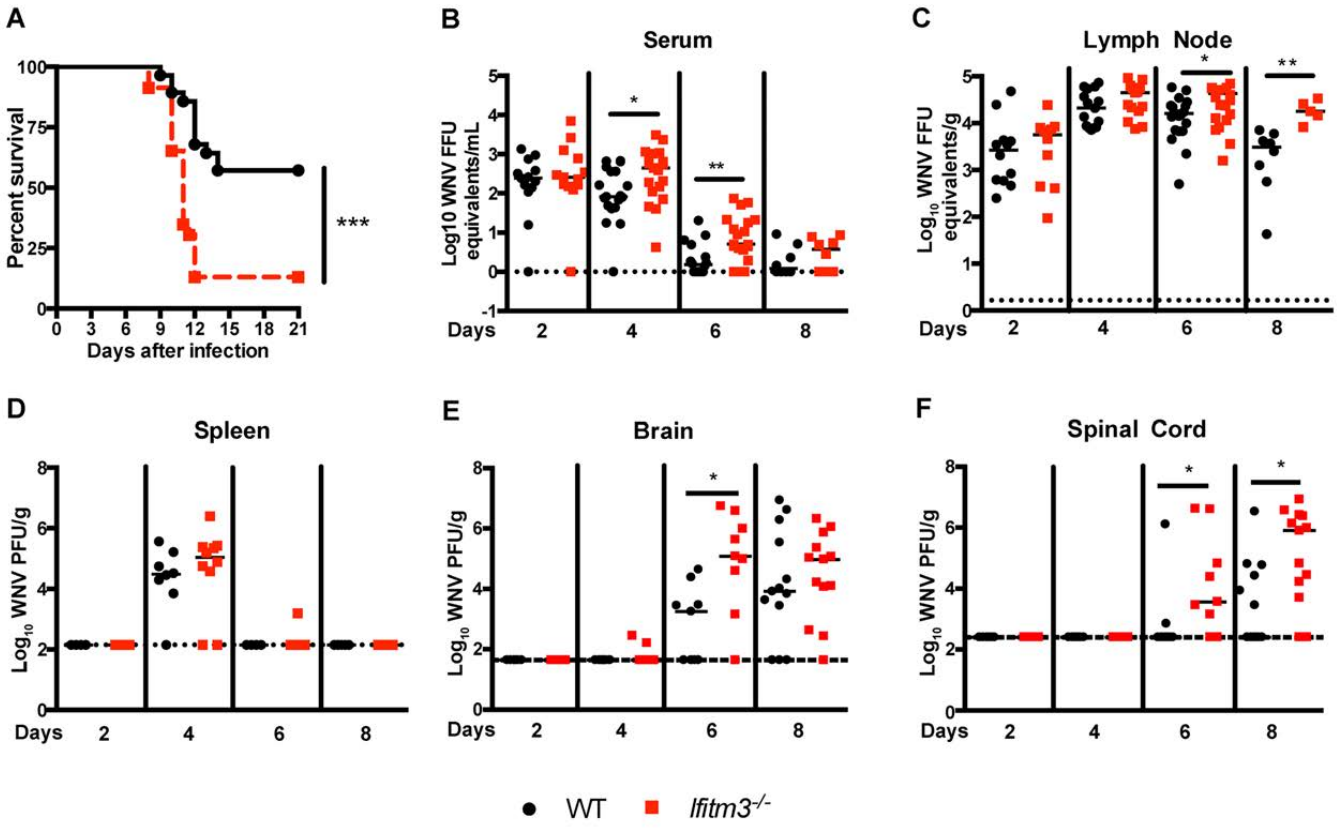

Journal of Virology

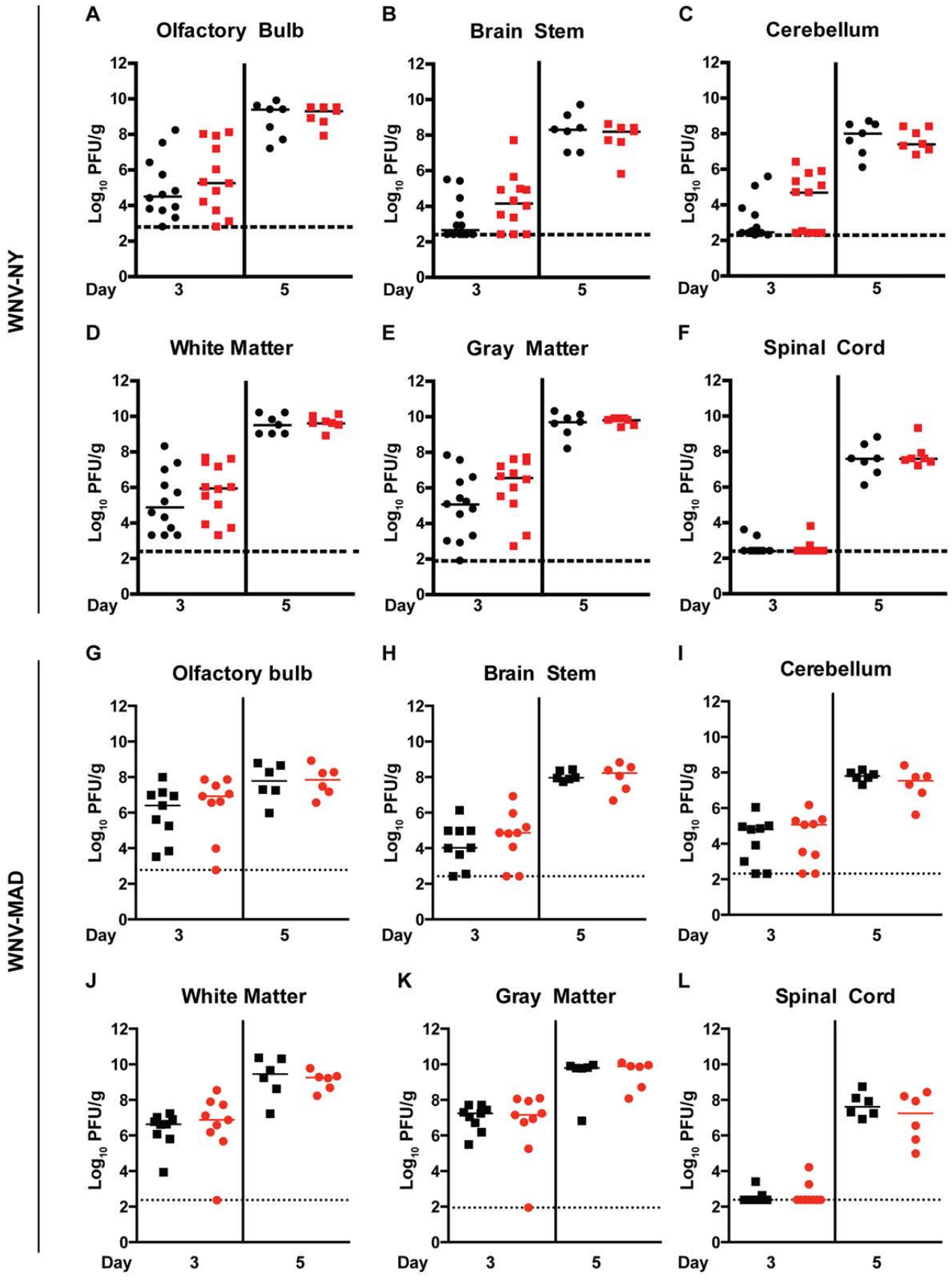

Journal of Virology

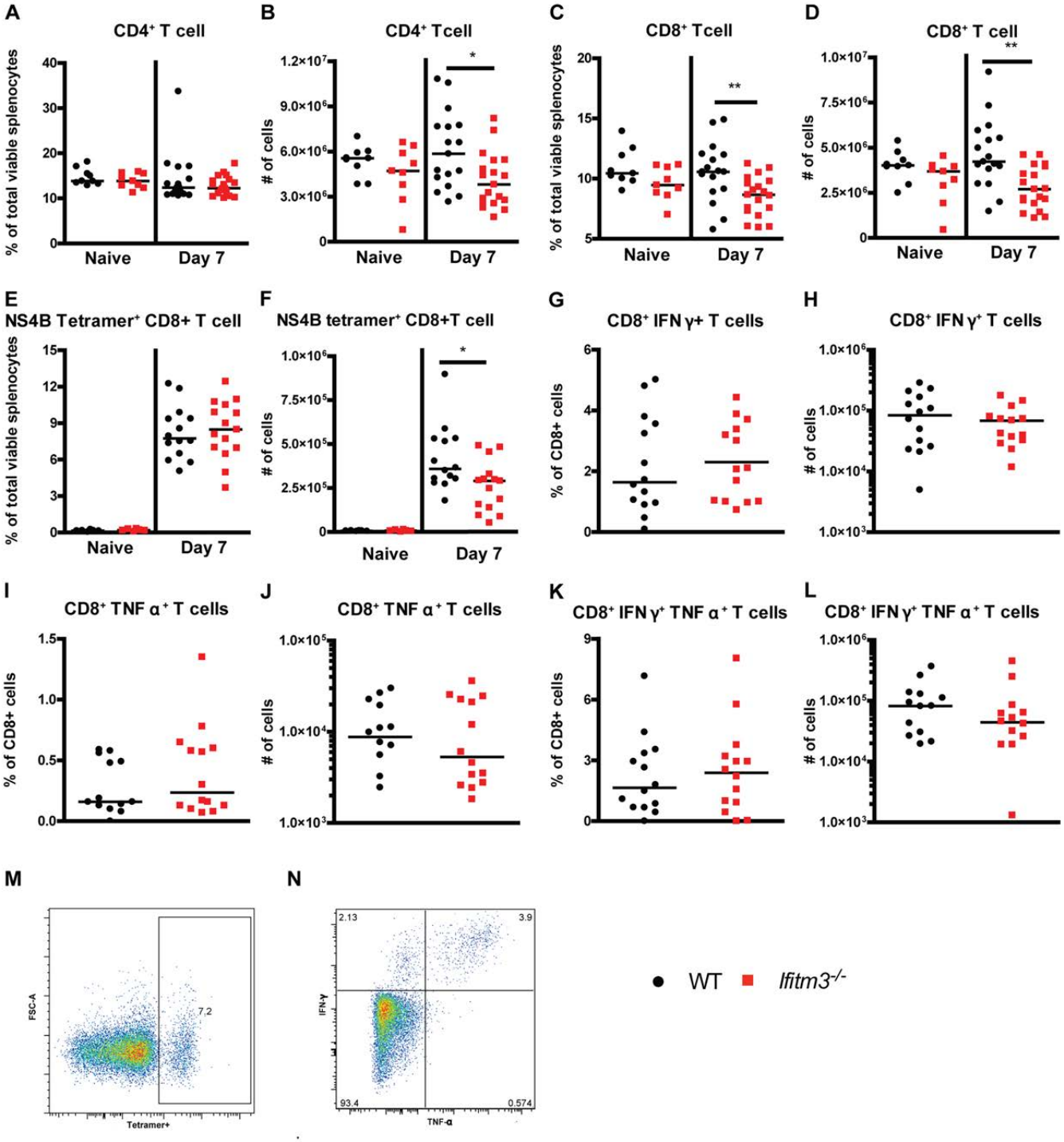

Journal of Virology